The p25 subunit of the dynactin complex is required for dynein–early endosome interaction

Jun Zhang,[1,2] Xuanli Yao,[1,2] Lauren Fischer,[1] Juan F. Abenza,[3] Miguel A. Peñalva,[3] and Xin Xiang[1,2]

[1]Department of Biochemistry and Molecular Biology and [2]Center for Neuroscience and Regenerative Medicine, the Uniformed Services University, Bethesda, MD 20814
[3]Departamento de Medicina Molecular y Celular, Centro de Investigaciones Biológicas, Consejo Superior de Investigaciones Cientificas, Madrid 28040, Spain

Cytoplasmic dynein transports various cellular cargoes including early endosomes, but how dynein is linked to early endosomes is unclear. We find that the *Aspergillus nidulans* orthologue of the p25 subunit of dynactin is critical for dynein-mediated early endosome movement but not for dynein-mediated nuclear distribution. In the absence of NUDF/LIS1, p25 deletion abolished the localization of dynein–dynactin to the hyphal tip where early endosomes abnormally accumulate but did not prevent dynein–dynactin localization to microtubule plus ends. Within the dynactin complex, p25 locates at the pointed end of the Arp1 filament with Arp11 and p62, and our data suggest that Arp11 but not p62 is important for p25–dynactin association. Loss of either Arp1 or p25 significantly weakened the physical interaction between dynein and early endosomes, although loss of p25 did not apparently affect the integrity of the Arp1 filament. These results indicate that p25, in conjunction with the rest of the dynactin complex, is important for dynein–early endosome interaction.

Introduction

Intracellular membrane trafficking is essential for cell function, and how motor proteins are targeted to various membranous cargoes to power their movement is a question of significant interest to the cell biology field (Caviston and Holzbaur 2006; Soldati and Schliwa 2006; Akhmanova and Hammer 2010). The minus end–directed cytoplasmic dynein motor transports organelles and vesicles along microtubules to their proper subcellular locations, and defects in dynein function are causally linked to multiple neurodegenerative diseases (Perlson et al., 2010). Early endosomes are among the cargoes of the dynein motor, and dynein-mediated retrograde transport of Rab5-associated early endosomes is crucial for neuronal growth and survival (Delcroix et al., 2003). However, it is unclear how a Rab5-associated early endosome interacts with the dynein motor.

The dynactin complex is important for a variety of cytoplasmic dynein functions in vivo, including mitosis, vesicle transport, nuclear positioning, and spindle orientation (Schroer 2004; Kardon and Vale 2009), but whether it is involved in targeting the dynein motor to membranous cargoes has been a recent issue of debate (Haghnia et al., 2007). Within the dynactin complex, the Arp1 (actin-related protein 1) subunit forms an actin-like mini-filament of 37 nm, which is the backbone of the complex. One end of the Arp1 filament is associated with the barbed-end capping protein, and the other end binds to the pointed-end complex that contains Arp11, p62, p25, and p27 (Schafer et al., 1994; Eckley et al., 1999; Hodgkinson et al., 2005; Imai et al., 2006). The p150 subunit, together with p50 and p24, forms a shoulder/sidearm complex, which locates on the top of the Arp1 polymer. The p150 protein of dynactin increases dynein processivity (King and Schroer 2000; Culver-Hanlon et al., 2006; Kardon et al., 2009), and directly binds to the dynein intermediate chain (Karki and Holzbaur 1995; Vaughan and Vallee 1995). Arp1 interacts with spectrin-like proteins, and thus, the Arp1 filament has been thought to link the dynactin complex and its associated dynein complex to membranous cargoes (Holleran et al., 1996, 2001; Muresan et al., 2001). Recently, spectrin mutations in *Drosophila melanogaster* have been shown to also cause defective axonal transport and neuronal degeneration (Lorenzo et al., 2010), which supports the importance of this interaction. However, a biochemical

J. Zhang and X. Yao contributed equally to this paper.

Correspondence to Xin Xiang: xxiang@usuhs.mil

L. Fischer's present address is PhD Program of Immunology, Microbiology and Virology, University of Rochester Medical Center, Rochester, NY 14642.

J.F. Abenza's present address is the Gurdon Institute, University of Cambridge, Cambridge CB2 1QN, England, UK.

Abbreviations used in this paper: ORF, open reading frame; UTR, untranslated region.

The Rockefeller University Press $30.00
J. Cell Biol. Vol. 193 No. 7 1245–1255
www.jcb.org/cgi/doi/10.1083/jcb.201011022

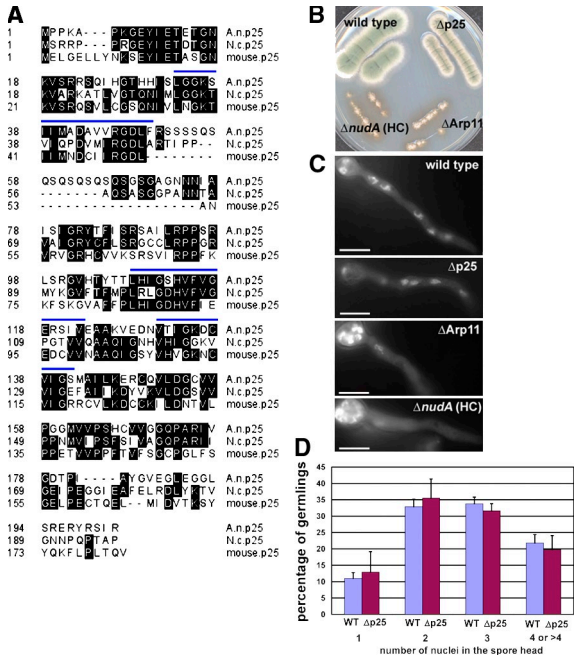

Figure 1. **The Δp25 mutant in *A. nidulans* does not exhibit a nud phenotype.** (A) Protein sequence alignment of p25 proteins from *A. nidulans* (A.n.p25), *N. crassa* (N.c.p25; Lee et al., 2001), and mouse (Eckley et al., 1999). Identical amino acids are boxed in black. Blue lines indicate Hexapeptide repeats in *A. nidulans* p25 identified using the Simple Modular Architecture Research Tool (SMART) program. (B) The Δp25 mutant grows slightly more slowly than the wild type on plates but is much healthier than a typical *nud* mutant such as Δ*nudA* (dynein heavy chain or HC) or ΔArp11. (C) Unlike the Δ*nudA* and ΔArp11 mutants, the Δp25 mutant exhibits normal nuclear distribution. The strains were grown in liquid Y + UU medium for 7.5 h at 37°C before being fixed and stained with DAPI for visualizing the nuclei. Bars, 5 µm. (D) A quantitative analysis of nuclear distribution in the Δ25 mutant in comparison to that in a wild-type control strain. More than 200 germ tubes were analyzed for each strain. Means and standard deviations (error bars) were calculated from three experiments. No significant differences are revealed at the P-value of 0.05.

study showed that in Arp1-RNAi–treated *Drosophila* S2 cells, although dynactin cannot be fully assembled and vesicle transport is defective, dynein's association with membrane compartments is not affected (Haghnia et al., 2007). Thus, it needs to be clarified whether Arp1 and its associated dynactin complex are important for targeting dynein to membranous cargoes.

In this study, we address the function of the dynactin complex in dynein–early endosome interaction in the filamentous fungus *Aspergillus nidulans*. In filamentous fungi, dynein and its regulators are important for nuclear distribution along elongated hyphae and also for the microtubule minus end–directed movement of early endosomes away from the tip (Morris 2000; Steinberg 2007; Peñalva 2010; Xiang and Oakley 2010). A previous study in *Neurospora crassa* showed that among the dynactin components analyzed, p25 at the pointed end of the Arp1 filament is the only protein that is required for vesicle transport but not for nuclear distribution (Lee et al., 2001). Here we studied the role of p25 in early endosome transport, and our current results strongly suggest that p25 and its associated dynactin complex are important for dynein to interact with early endosomes.

Results

Deletion of the *A. nidulans* p25 orthologue impairs movement of early endosomes but not nuclear distribution

We identified the p25 orthologue in the *A. nidulans* genome (An5022) by using the *N. crassa* p25 protein (Lee et al., 2001) as a query (http://www.broadinstitute.org/annotation/genome/aspergillus_group/MultiHome.html). *A. nidulans* p25 contains 202 amino acids with a predicted molecular weight of 21 kD. It shows significant sequence identity with p25 proteins from both *N. crassa* (197 amino acids, 21 kD; Lee et al., 2001) and mouse (182 amino acids, 20 kD; Eckley et al., 1999) with E-values of 7.6×10^{-43} and 4.37375×10^{-23}, respectively (Fig. 1 A). Sequence analysis suggests that p25 forms a left-handed β helix and contains hexapeptide repeats (Parisi et al., 2004). *A. nidulans* p25 also contains several characteristic hexapeptide repeats (Fig. 1 A).

We constructed a deletion allele of p25, Δp25, in *A. nidulans* (Fig. S1). Δp25 mutant colonies grown on plates appeared much healthier than Δ*nudA* (dynein heavy chain or HC) and ΔArp11 mutants, which exhibited a characteristic nud (nuclear distribution) colony phenotype characterized by small colony size and the lack of asexual spores (conidia; Fig. 1 B). The colony diameter of the Δp25 mutant was ∼66% of the wild type, whereas those of the Δ*nudA* or ΔArp11 mutants were only ∼15–20% of the wild type. Conidia (asexual spores) were present on top of the colony as judged by the color of the colony (which comes from conidia) although conidiation (asexual spore production) seemed less robust than in the wild type as the color of the colony is dimmer (Fig. 1 B). In contrast with loss-of-function mutations affecting the other dynactin components such as p150, Arp1, Arp11, p62, and p50, all of which produce a nud phenotype as indicated by clustering of multiple nuclei in the spore head of the germ tube (Zhang et al., 2003, 2008), nuclear distribution appeared normal in the Δp25 cells (Fig. 1 C). A quantitative analysis of nuclear distribution was performed for wild type and the Δp25 mutant by counting the number of nuclei in the spore head of germ tubes. Our results show that there is no significant difference in the nuclear distribution patterns between wild type and the mutant (Fig. 1 D).

We then determined if p25 is required for dynein-mediated early endosome movement. In filamentous hyphae, dynein powers the minus end–directed movement of early endosomes (Steinberg and Schuster 2011). Defects in dynein and its regulators—dynactin and NUDF/LIS1—cause an abnormal buildup of early endosomes at the hyphal tip where microtubule plus ends locate (Lenz et al., 2006; Abenza et al., 2009; Zhang et al., 2010). In *A. nidulans*, RabA-associated early endosomes were observed using GFP-RabA and mCherry-RabA fusion proteins (Abenza et al., 2009; 2010). In wild-type cells, bidirectional movements of RabA-containing early endosomes were observed in time-lapse sequences (Video 1; Abenza et al., 2009). In still images, early endosomes were seen to distribute along the hyphae (Fig. 2 A). In the Δp25 mutant, however, a very conspicuous, abnormal accumulation of mCherry-RabA-labeled early endosomes at the hyphal tip was seen (Fig. 2 A and

Videos 2 and 3). This phenotype is similar to that exhibited by the *nudA* dynein heavy chain mutants (Abenza et al., 2009; Zhang et al., 2010), including the Δ*nudA* mutant (Fig. 2 A and Video 4), which indicates that p25 is critical for dynein-mediated basipetal movement of early endosomes. Because endocytosis is coupled to hyphal tip growth (Araujo-Bazán et al., 2008; Taheri-Talesh et al., 2008; Upadhyay and Shaw 2008; Harris 2010; Hervas-Aguilar and Peñalva, 2010), and the Δ*nudA* mutant grows more slowly than the Δp25 mutant, the hyphal tip accumulation of mCherry-RabA signals in the Δp25 cells even appeared more prominent than that in the Δ*nudA* mutant. Some mCherry-RabA dots behind the hyphal tip in Δp25 mutant were observed, but most of them do not undergo directional movements. We did notice that some mCherry-RabA dots in wild-type hyphae do not undergo directional movements either. We quantified the frequency of movements within 10 µm of the hyphal tip by measuring the numbers of dots moving toward and away from the hyphal tip where microtubule plus ends locate. As expected, loss of p25 dramatically decreased the frequency of movements away from the tip (Fig. 2 B). Intriguingly, loss of p25 also caused a dramatic decrease in the frequency of movements toward the tip (Fig. 2 B), a phenomenon that we currently do not fully understand, but may indicate that anterograde membrane trafficking is coupled to retrograde membrane trafficking.

In fungi, GFP-labeled dynein molecules form dynamic comet-like structures representing their accumulation at the microtubule plus ends (Han et al., 2001; Lee et al., 2003; Sheeman et al.,2003; Lenz et al.,2006). Because the plus-end localization of dynein in filamentous hyphae facilitates retrograde movements of early endosomes (Lenz et al., 2006; Abenza et al., 2009; Zekert and Fischer 2009), we tested the effect of p25 deletion on dynein localization by introducing the GFP–dynein heavy chain (or GFP-HC) fusion into the Δp25 mutant via crossing. Plus-end comets formed by GFP-HC could clearly be observed in the Δp25 mutant (Fig. 2 C), although the mean signal intensity of the comets as measured was ∼65% of the wild type (Fig. 2 D; $P < 0.01$). Thus, compared with the almost complete elimination of dynein comets in mutants of other dynactin components such as p150, Arp1, Arp11, p62, and p50 (Zhang et al., 2003, 2008; Lenz et al., 2006), the effect of Δp25 on dynein comets is relatively minor. It should be noted that plus-end localization of dynein is not a prerequisite for motor activation (Zhang et al., 2010). Although this enrichment of dynein at the plus ends facilitates dynein–early endosome interaction, dynein molecules along microtubules are still able to move cargoes (Schuster et al., 2011a,b). In *Ustilago maydis*, a 50% reduction of dynein accumulation at the plus ends caused by blocking EB1–dynactin interaction causes a low percentage (∼10%) of early endosomes to fall off the microtubule track at the plus ends but does not cause any significant accumulation of early endosomes at the hyphal tip (Schuster et al., 2011a). Therefore, although the reduction of the *A. nidulans* HC's plus-end accumulation in Δp25 cells may contribute to the endosome motility defect to certain extent, it cannot fully explain the dramatic accumulation of early endosomes at the hyphal tip and that

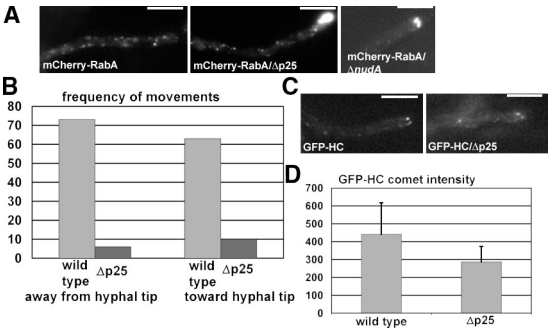

Figure 2. **Dynein-mediated retrograde movement of early endosomes is significantly impaired in the Δp25 mutant, although dynein is still able to concentrate at microtubule plus ends.** (A) mCherry-RabA–labeled early endosomes move and distribute along the wild-type hyphae, whereas they accumulate as a cloud at the hyphal tip in the Δp25 mutant and in the Δ*nudA* mutant. (B) A quantitative analysis of the frequency of movements toward or away from the hyphal tip. Because microtubules have mixed polarity in the multi-nucleate hyphae, we only focused on the small region within 10 µm behind the hyphal tip, where most of the plus ends of microtubules should face the hyphal tip. This experiment was done once with data combined from a total of 30 time-lapse sequences from the wild-type cells and a total of 30 time-lapse sequences from the Δp25 cells. For each time-lapse sequence, 30 frames were taken with a 0.1-s exposure time and a 0.3-s interval between frames. Frequency of movements in a total of 360 s is shown. (C) In both the wild type and the Δp25 mutant, GFP-labeled dynein heavy chains (HC) form comet-like structures representing their microtubule plus-end accumulation. Bars, 5 µm. (D) Mean and standard deviation values (error bars) of maximal signal intensity (arbitrary units) of the plus-end GFP-HC comets in Δp25 cells and wild-type cells are shown ($n = 14$, $P < 0.01$).

the frequency of movements away from the hyphal tip in wild type cells is >10 fold of that in the Δp25 mutant (Fig. 2, A and B). This notion prompted us to further test the role of p25 in the interaction between dynein and early endosomes.

In NUDF/LIS1-depleted cells, p25 is required for the localization of dynein and dynactin to the hyphal tip region where early endosomes accumulate

In Δ*nudF* cells, GFP-HC forms a cloud-like structure at the hyphal tip where early endosomes also accumulate (Fig. 3 A and Videos 5–7; Zhang et al., 2010). Although the nature of this cloud-like hyphal tip accumulation of dynein is not clear, as it largely but not fully overlaps with the early endosome signals (Fig. 3 A and Videos 5–7), it most likely reflects dynein localization to the aggregate of early endosomes and/or other dynein cargoes accumulated in the same region. In *alcA-nudF* cells grown on glucose, a repressive condition that shuts off NUDF expression, GFP-HC and p150-GFP form a cloud-like structure at a large majority (70% or more) of hyphal tips (Fig. 3, B and C; and Video 8). However, in the absence of p25, we have never found a single *alcA-nudF* cell that showed the cloud-like structure formed by GFP-HC and p150-GFP molecules at the hyphal tip, although comet-like structures are present and early endosomes are also accumulated at the hyphal tip in the same mutant background (Fig. 3, B–D). These results suggest that p25 is required for dynein/dynactin localization to the hyphal tip region where early endosomes and possibly other dynein cargoes are accumulated.

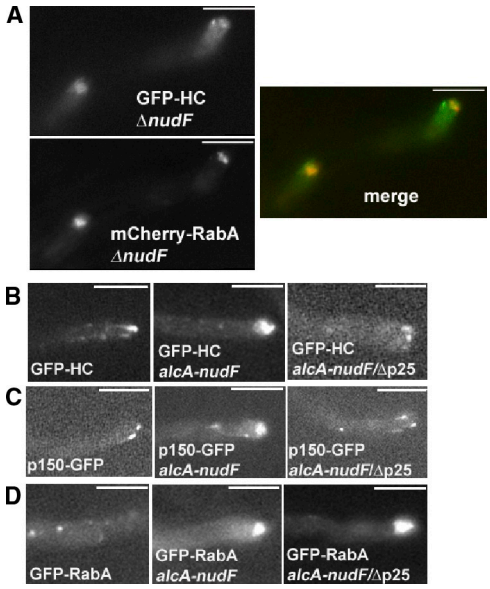

Figure 3. **In NUDF-depleted cells, p25 is required for the localization of dynein (GFP-HC) and dynactin (p150-GFP) to the hyphal tip region, where early endosomes are enriched.** (A) Images showing that in the same *ΔnudF* cells, both GFP-HC and mCherry-RabA localize to the hyphal tip region. (B–D) In NUDF-depleted cells (*alcA-nudF* grown on glucose), p25 is required for the localization of dynein and dynactin to the hyphal tip region where early endosomes are found. Images of GFP-HC (B), p150-GFP (C), and GFP-RabA (D) are shown. In the absence of NUDF (*alcA-nudF*), a portion of GFP-HC and p150-GFP proteins localize to the hyphal-tip region, where early endosomes also accumulate (B–D, middle). Introducing the Δp25 mutant allele into this background (*alcA-nudF*/Δp25) abolishes this hyphal tip accumulation but maintains the plus-end comets of GFP-HC and p150-GFP (B and C, right). Bars, 5 µm.

p25 and the dynactin complex are important for the physical interaction between the dynein complex and early endosomes

We developed a biochemical assay to determine if p25 and the dynactin complex are required for the physical interaction between early endosomes and dynein. We created strains coexpressing the S-tagged dynein intermediate chain (S-IC) and GFP-RabA. Cell extracts were prepared in the absence of detergent and incubated with S-protein agarose beads, which were washed gently and eluted with S-peptide as described previously (Zhuang et al., 2007). In the absence of detergent, a fraction of dynein molecules should be bound to early endosomes, and thus GFP-RabA, which specifically labels early endosomes, should be found in the eluate. To determine if the dynactin complex is important for dynein–early endosome interaction, we used extracts from *alcA-nudK*^{Arp1} (or *alcA*-Arp1) cells grown on glucose-containing repressing medium (YUU). In the *alcA*-Arp1 cells, p150 levels decrease dramatically when Arp1 expression is repressed (Zhang et al., 2008), which should impair dynein–dynactin interaction because p150 is the dynactin subunit that interacts with dynein (Karki and Holzbaur 1995; Vaughan and Vallee 1995). We found that although S-IC pulls down GFP-RabA from wild-type cell extracts, the amount of pulled-down GFP-RabA from Arp1-depleted cells is significantly decreased ($P < 0.001$; Fig. 4, A and B). To confirm that this is not caused by a decreased protein level of GFP-RabA in the mutant, we performed a Western blot analysis on the extracts used for the pull-down assay, and found that the protein levels of GFP-RabA are similar in the wild type and the *alcA*-Arp1 cells (Fig. 4 C). Together, these data strongly indicate that dynactin is important for linking dynein to early endosomes. We then determined the role of p25 in the physical interaction between dynein and early endosomes using the same assay. We used a strain containing the S-IC, Δp25, and GFP-RabA alleles to determine the levels of RabA pulled down by S-IC in the absence of p25. Compared with the wild type, the amount of pulled-down GFP-RabA proteins from the Δp25 mutant cell extract was significantly decreased ($P < 0.001$; Fig. 4, D and E). This decrease is not caused by the presence of lower levels of GFP-RabA in the mutant extract (Fig. 4 F). Thus, p25 plays an important role in the linkage between dynein and early endosomes. Our data also suggest that the extent of decrease in dynein–early endosome interaction caused by Δp25 is not significantly different from that caused by loss of Arp1 (at $P = 0.05$).

Loss of p25 does not significantly affect the Arp1 filament

Loss of p25 does not affect nuclear distribution, which suggests that the rest of the dynactin complex is intact in its absence. For example, Arp11 and p62 must be functional in the Δp25 mutant because loss of either one of them prevents normal nuclear distribution (Lee et al., 2001; Zhang et al., 2008). In Arp11-depleted cells, S-tagged p150 pulled down significantly less Arp1, which suggests that in the absence of Arp11, the Arp1 filament consisting of multiple Arp1 subunits may be shortened and/or that the interaction between p150 and Arp1 is weakened (Fig. S2; Zhang et al., 2008). In marked contrast, in the Δp25 mutant the amount of pulled-down Arp1 was similar to that of the wild type (Fig. 5, A and B; and Fig. S2). Together, these results indicate that the effect of p25 deletion on dynein–early endosome interaction is unlikely to be caused by any significant alteration of the Arp1 filament. In addition, loss of p25 does not negatively affect dynein–dynactin interaction (Fig. S3), showing that the effect of p25 deletion on dynein–early endosome interaction is not caused by a loss of dynein–dynactin interaction.

Because loss of *A. nidulans* p25 does not significantly affect the integrity of the dynactin complex, we performed the following experiment to confirm that the *A. nidulans* p25 is indeed a component of the dynactin complex. We constructed a strain in which the expression of the p25–GFP fusion is under the control of the native p25 promoter and determined the localization of p25-GFP. As expected for a component of the dynactin complex, p25-GFP forms benomyl-sensitive comet-like structures (Fig. 5 C) resembling those previously seen with other dynein and dynactin components at the microtubule plus ends (Han et al., 2001; Zhang et al., 2003). Most interestingly, Western analyses showed that the p25-GFP protein levels are dramatically decreased in Arp11-depleted cells but not in p62-depleted cells (Fig. 5 D). This result suggests that the *A. nidulans* p25 depends on Arp11, rather than p62, to associate with the dynactin complex, and that

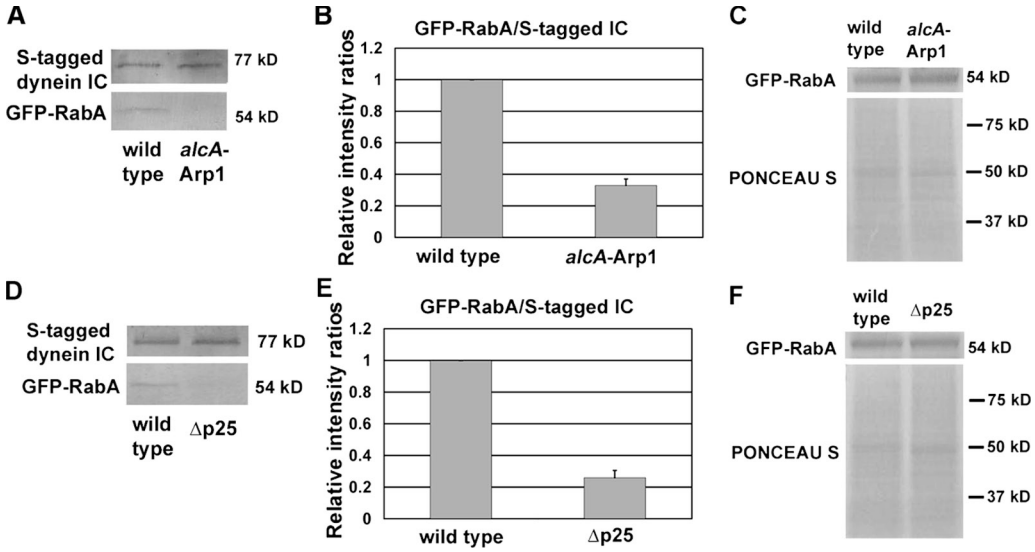

Figure 4. **p25 and its associated dynactin complex are important for the physical interaction between dynein and early endosomes.** (A) Although S-tagged dynein IC was able to pull down GFP-RabA in wild-type extracts in the absence of detergent, the amount of pulled-down GFP-RabA in Arp1-depleted extracts was significantly decreased. (B) A quantitative analysis of the Western results. All the values were relative to wild-type values, which were set as 1. Mean and standard deviation values were based on results from three independent pull-down experiments ($P < 0.001$). (C) The protein levels of GFP-RabA in the wild type and *alcA*-Arp1 extracts were similar before the pull-down assay. (D) Although S-tagged dynein IC was able to pull down GFP-RabA in wild-type extracts in the absence of detergent, the amount of pulled-down GFP-RabA in Δp25 extracts was significantly decreased. (E) A quantitative analysis of the Western results. All the values were relative to wild-type values, which were set as 1. Mean and standard deviation values (error bars) were based on results from three independent pull-down experiments ($P < 0.001$). (F) The protein levels of GFP-RabA in the wild-type and Δp25 extracts were similar before the pull-down assay.

the p25 protein is not stable when this association is impeded. In agreement with this suggestion, loss of p62 has no negative effect on the binding of p25 to the dynactin complex as the S-tagged p150 of dynactin is able to pull down p25-GFP from p62-depleted cell extracts as efficiently as from wild-type extracts (Fig. 5 E).

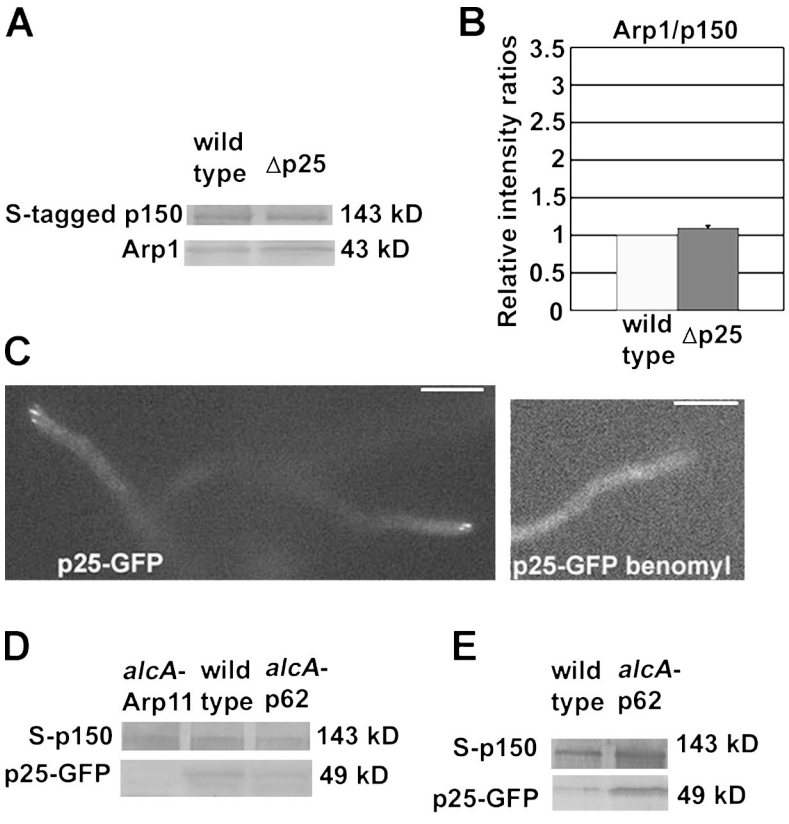

Figure 5. **Although loss of p25 has no apparent effect on the Arp1 filament, the *A. nidulans* p25 is indeed a component of the dynactin complex.** (A) Western blots showing Arp1 proteins pulled down by the S-tagged p150 in wild-type and Δp25 extracts. (B) A quantitative analysis of the Western results on p150–Arp1 interaction in the Δp25 mutant. All the values were relative to wild-type values, which were set as 1. Mean and standard deviation values (error bars) were based on results from three independent experiments. At $P = 0.05$, there is no significant difference between wild-type and Δp25 values. (C) p25-GFP forms benomyl-sensitive comet-like structures, consistent with being a component of the dynactin complex. For treatment with benomyl to depolymerize microtubules, 2.4 μg/ml of benomyl was used to treat the cells for 20 min. Bars, 5 μm. (D) A Western blot showing that the p25-GFP protein level was dramatically decreased in Arp11-depleted cells but not in p62-depleted cells. (E) S-tagged p150 was able to pull down p25-GFP from both the wild type and the p62-depleted extracts.

Discussion

Although dynein is known to be involved in the transport of a variety of membranous cargoes, how the motor is targeted to these cargoes is still a topic under investigation. In filamentous fungi and higher eukaryotic cells such as neurons, early endosomes undergo dynein-mediated transport, but how dynein is targeted to these vesicles is unclear (Akhmanova and Hammer 2010; Peñalva 2010). Our current data from the fungal model *A. nidulans* strongly suggest that p25 and its associated dynactin complex play a crucial role in linking dynein to early endosomes in vivo.

The dynactin complex physically interacts with the dynein complex through direct binding between p150 of dynactin and the dynein IC (Karki and Holzbaur 1995; Vaughan and Vallee 1995). It is thought that the dynactin complex facilitates dynein function by two different mechanisms. First, the p150 subunit of the dynactin complex enhances dynein processivity along microtubules, although whether this function is mediated via the microtubule-binding domain of p150 is a matter of dispute (King and Schroer 2000; Culver-Hanlon et al., 2006; Kim et al., 2007; Dixit et al., 2008; Kardon et al., 2009; Moore et al., 2009a). Second, the Arp1 filament within the dynactin complex is thought to mediate the physical interaction between dynactin and membranous cargoes, thereby targeting dynein to membranous organelles (Holleran et al., 1996, 2001; Muresan et al., 2001; Schroer 2004). However, this idea has been under debate recently, mainly because results from a study in *Drosophila* S2 cells argue against a role of Arp1 in dynein–membrane interaction (Haghnia et al., 2007). Although knocking down Arp1 using RNAi did impair the transport of membranous cargoes, it did not appear to affect dynein–membrane interaction as judged by a membrane-flotation assay (Haghnia et al., 2007). Because loss of Arp1 leads to disruption of the dynactin complex and also to a significant decrease in the level of the dynein-interacting p150 subunit both in *Drosophila* S2 cells and in filamentous fungi (Minke et al., 1999; Haghnia et al., 2007; Zhang et al., 2008), this study not only questions the role of Arp1 but also questions the role of the dynactin complex in targeting dynein to membranous cargoes.

Our current data strongly indicate the importance of the dynactin complex in linking dynein to early endosomes. In our biochemical experiments, we have examined specifically the association between dynein and early endosomes rather than the interaction of dynein with general membranous materials. This possibly explains the discrepancy between our conclusions and those of the earlier study in *Drosophila* S2 cells, in which the "general" dynein–membrane interaction was examined, as it is possible that dynactin is required for targeting dynein to some but not all the membranous cargoes. For example, the interaction between dynein and rhodopsin-carrying vesicles occurs in a dynactin-independent manner via the physical interaction between the Tctex-1 dynein light chain and the C-terminal cytoplasmic tail of rhodopsin (Tai et al., 1999). A recent study in *Xenopus* melanophores indicated that CLIP-170 at the microtubule plus end captures melanosomes in a dynactin-independent manner for their dynein-dependent minus end–directed transport (Lomakin et al., 2009). Previously, the C-terminal region of $p150^{Glued}$ dynactin has been implicated in the interaction between dynein and Rab7-marked late endosomes (Johansson et al., 2007), but a recent study indicates that in neuronal cells the direct interaction between dynein intermediate chain and Snapin is important for late endosome movement (Cai et al., 2010). In addition, the interaction between dynein and Rab11-containing recycling endosomes seems to be mediated by the dynein light intermediate chain (Horgan et al., 2010), and the dynein LC8 light chains are responsible for linking dynein to Piccolo-Bassoon transport vesicles (Fejtova et al., 2009). It is also interesting to note that the mitotic checkpoint protein ZW10 recruits dynein not only to kinetochores, but also to ER-Golgi membranes (Vallee et al., 2006). This recruitment may be mediated by the ZW10-dynamitin (p50 of dynactin) interaction as indicated by yeast two-hybrid analysis (Starr et al., 1998), or by a direct interaction between ZW10 and phosphorylated dynein intermediate chain, which recruits dynein to kinetochores before metaphase (Whyte et al., 2008). Finally, interaction between dynein and the membranous spindle matrix is mediated by a dynein-interacting protein Nudel (Ma et al., 2009), Given the variety of targeting mechanisms used by different populations of vesicles and membranous structures, it is important to address specifically the interaction of dynein with any specific class of membranous organelles.

Our current work not only demonstrates the importance of the dynactin complex in targeting dynein to early endosomes, but it also uncovers a specific role of the p25 component of dynactin in dynein–early endosome interaction. In a previous study in *N. crassa*, p25 was found not to be required for the interaction between dynein and membranes, and indeed deletion of p25 appeared to strengthen dynein–membrane interaction (Lee et al., 2001). Because a general membrane-flotation assay was used in the *N. crassa* study, whereas a specific dynein–early endosome interaction assay was used in our study, we think that, as discussed earlier, p25 is required for dynein to interact with a subset but not all membranous vesicles. It should be pointed out that although our study points out an important role of p25 in dynein–early endosome interaction, our data do not exclude the possibility that p25 may cooperate with other dynactin components, such as Arp1, to interact with early endosomes. Because different dynactin components affect each other within the complex, it is not straightforward to use knockout or knockdown methods to address the specific roles of every dynactin components in the dynein–early endosome interaction. For example, the Arp1 protein is the backbone of the dynactin complex, and its loss leads to a disruption of the whole complex. In *Drosophila* and in filamentous fungi such as *N. crassa* and *A. nidulans*, loss of Arp1 results in a dramatic decrease in the protein level of p150 (Minke et al., 1999; Haghnia et al., 2007; Zhang et al., 2008), the key component of dynactin that mediates the interaction between dynein and dynactin (Karki and Holzbaur 1995; Vaughan and Vallee 1995). In addition, loss of other Arp1 pointed-end proteins such as Arp11 and p62 significantly lowers the levels of Arp1 pulled down by S-tagged p150, which suggests that these proteins are required for the integrity of the Arp1 filament and/or for the p150–Arp1 interaction. Moreover, loss of function of many dynactin components, such as p150,

Arp1, Arp11, p62, and p50, causes a dramatic defect in dynein localization to the microtubule plus ends, as dynein comets are either completely absent or extremely hard to be observed in the mutants (Zhang et al., 2003; Lenz et al., 2006; Zhang et al., 2008), which should lead to a defect in dynein–early endosome interaction. However, loss of p25 does not apparently disrupt the function of the core complex because nuclear distribution is completely normal in the p25-null mutant. The idea that the absence of p25 does not apparently affect either the Arp1 filament or other pointed-end proteins is also supported by the results of our biochemical experiments. Although loss of Arp11 or p62 significantly reduced the amount of Arp1 pulled down by p150 (Zhang et al., 2008), loss of p25 does not produce this effect. Although we would not exclude the possibility that p25 may affect the dynactin complex in a subtle way that may contribute to the defect of dynein–early endosome interaction, our data strongly support the conclusion that p25, when associated with the dynactin complex, plays a significant role in dynein–early endosome interaction.

In the vertebrate dynactin complex, p25 forms a complex with p27, Arp11, and p62 at the pointed end of the Arp1 filament (Schroer 2004). It is interesting to note that some or all of these four pointed-end components may be missing in some eukaryotic organisms. For example, *Saccharomyces cerevisiae* does not contain obvious orthologues of p25, p27, and p62 (Eckley et al., 1999; Moore et al., 2008), which is consistent with the known function of *S. cerevisiae* dynein in nuclear migration/spindle orientation but not vesicle transport (Yeh et al., 1995; Moore et al., 2009b). Interestingly, no sequence homologues of these three components are found in the database of *Schizosaccharomyces pombe* either. Moreover, although *S. cerevisiae* contains the Arp11 orthologue Arp10 (Clark and Rose 2006; Moore et al., 2008), we could not confidently conclude if *S. pombe* contains a true Arp10/Arp11 orthologue, as the mouse Arp11 protein shows higher homology with other Arps in the *S. pombe* genome than with the candidate Arp10 protein. As Arp11 in *A. nidulans* and Arp10 in *S. cerevisiae* have similar functions in regulating the Arp1 filament (Moore, et al., 2008; Zhang et al., 2008), one may predict that a true Arp11 orthologue in *S. pombe* will most likely play a similar role. In *A. nidulans*, Arp11, p62, and p25 are present, and a putative p27 orthologue (An11815, $E = 3.7 \times 10^{-2}$ with mouse p27) has also been found. Our previous result obtained from imaging GFP-p62 in the ΔArp11 mutant suggested that p62 depends on Arp11 to associate with the rest of dynactin complex (Zhang et al., 2008). Our current result suggests that p25 depends on Arp11 rather than p62 to associate with the dynactin complex, and the stability of p25 depends on Arp11 or its association with the complex. Thus, Arp11 must be at the most proximal position relative to the pointed end of the Arp1 filament, and it interacts with the Arp1 filament directly. This notion is consistent with the idea that in *S. cerevisiae*, only Arp10 is associated with the Arp1 filament, whereas all other pointed-end proteins are missing, and that the stability of Arp10 depends on the Arp1 filament (Clark and Rose 2006; Moore et al., 2008). All these four pointed-end proteins are present in *N. crassa* (Borkovich et al., 2004), *U. maydis*, and *Dictyostelium discoideum*. It would be important to investigate and compare the functions of these pointed-end proteins in the transport of various organelles in a variety of organisms.

Materials and methods

Strains and media

A. nidulans strains used in this study are listed in Table I. For biochemical experiments involving dynactin isolation, YG (yeast extract plus glucose) + UU (or YUU) liquid medium was used. For DAPI staining of nuclei, YUU liquid medium was used. For live cell imaging experiments, minimal medium containing glucose or glycerol plus supplements was used.

Construction of the p25 deletion mutant

The p25 deletion (Δp25) construct was made using a fusion PCR strategy as described previously (Szewczyk et al., 2006). Specifically, the upstream region was amplified from wild-type genomic DNA using P25*u5′* (5′-CAACGAGTACACTATCTC-3′) and P25u3′ (5′-TGCTTTAGGCGGCATTTTG-3′), and the downstream region was amplified using P25d5′ (5′-ATCCGATAGGTACTGTAC-3′) and P25d3′ (5′-AGATATCGCCTATTACGGAC-3′). *Aspergillus fumigatus pyrG* used for replacing the coding region of p25 was amplified from the plasmid pAO81 (Yang et al., 2004) using AfpyrG*5′* (5′-CTATCAAAATGCCGCCTAAAGCATGCTCTTCACCCTCTTCG-3′) and AfpyrG3′ (5′-ACTCCAAGTACAGTACCTATCGGATCTGTCTGAGAGGAGGCAC-3′). The final linear Δp25 construct obtained by fusion PCR was transformed into the LZ12 strain that contains GFP-dynein HC under the control of its native promoter (Zhuang et al., 2007). Transformants were screened using PCR of genomic DNA to confirm the correct integration of the construct into the p25 locus. The primers used for verifying the correct integration were p25UU (p1; 5′-CGGAAATAAGGTCCATCCGC-3′), AFpyrG3 (p2; 5′-GTTGCCAGGTGAGGGTATTT-3′), AFpyrG*5* (p3; 5′-AGCAAAGTGGACTGATAGC-3′) and p25DD (p4; 5′-AACAAGAACATGAGAAACGA-3′). The result of the PCR analysis is shown in Fig. S1. p1 and p4 are not located within the flanking sequences of the Δp25 construct but just upstream and downstream of the sequences (Fig. S1 A). The 1 kb (with p1 + p2) and 1.1 kb (with p3 + p4) products were specifically produced using the genomic DNA isolated from the Δp25 mutant as template, which indicates that the integration occurred in a site-specific manner as expected (Fig. S1 B). The site-specific integration was also confirmed by a Southern blot analysis on XhoI-digested genomic DNAs using the 3′ flanking sequence of the Δp25 construct as a probe (Fig. S1, C and D). Moreover, the absence of other unexpected signals beside the 2.6 kb expected signal on the Southern blot suggests that the Δp25 construct only underwent a site-specific integration into the p25 locus in the Δp25 mutant strain (Fig. S1, C and D).

Construction of the p150-GFP strain

A C-terminal region of the *nudM* open reading frame (ORF) and the 3′ untranslated region (UTR; possibly also with sequences downstream of the *nudM* gene; 3′ UTR) were amplified from wild-type genomic DNA, with corresponding primer pairs of ORF forward (5′-GTTGCTACAGTGAAGATCAACCGTG-3′) and ORF reverse (5′-TAAGGTTGGTTTAATTGCTCGCTCA-3′), and UTR forward (5′-CAGACCTTTTCTATGGGCTGCTTAG-3′) and UTR reverse (5′-TTACCGTCATGAAGGCGACGAC-3′). The DNA containing GFP and an *A. fumigatus pyrG* gene (*AfpyrG*) was amplified from the pFNO3 plasmid (deposited to the Fungal Genetics Stock Center by Stephen A. Osmani, Ohio State University, Columbus, OH; Yang et al., 2004; McCluskey et al., 2010) with the fusion forward primer (5′-CAGCCTGTTGAGCGAGCAATTAAACCAACCTTAGGAGCTGGTGCAGGCGCTGGAG-3′) and the fusion reverse primer (5′-AGATGGCTAAGCAGCCCATAGAAAAGGTCTGCTGTCTGAGAGGAGGCACTGATG-3′). Note that the GFP tag follows an 8-aa linker GAGAGAGA. Thus, the fusion forward primer contains no GFP sequence but the nucleotide sequence encoding almost the entire linker (GGAGCTGGTGCAGGCGCTGGAG for amino acids GAGAGAGA). The resultant PCR product, GFP-Af*pyrG*, contains the GFP and the selective marker Af*pyrG*, and it also contains, at the 5′ and 3′ ends, respectively, 33- and 31-bp sequences derived from the *nudM* gene. A fusion PCR was first performed on the ORF and the GFP-Af*pyrG* fragments using the ORF forward and fusion reverse primers. The fusion product was then fused to the UTR after another fusion PCR using ORF-F2 (5′-GTCCTTTCAAGCAAGCAGAGAATG-3′) and UTR-R2 (5′-GATGCTGAGCTTGCTGCCTG-3′). The fusion fragment was transformed to the TNO2A3 strain (provided by B. Oakley, University of Kansas, Lawrence, KS; Nayak et al., 2006). Transformants

Table I. ***A. nidulans* strains used in this study**

Strain	Genotype	Source
JZ270	Δp25-Af*pyrG; argB2::[argB*-alcAp*::mCherry-*RabA]; pantoB*100; possibly Δ*nkuA::argB*	This paper
JZ291-294	Δp25-Af*pyrG;* S-tagged *nudM*-Af*pyrG*; possibly Δ*nkuA-argB*; possibly *pyrG*89	This paper
JZ350-351	GFP-*nudA*; *alcA-nudF-pyr4; pabaA1*	This paper
JZ352	Δp25-Af*pyrG; alcA-nudF-pyr4;* GFP-*nudA; pyroA*4	This paper
JZ359-361	*pyroA4[pyroA*-RabAp*::GFP-*RabA];* Δp25-Af*pyrG*	This paper
JZ362	*pyroA4[pyroA*-RabAp*::GFP-*RabA]; alcA-nudF-pyr4*	This paper
JZ366	*pyroA4[pyroA*-RabAp*::GFP-*RabA];* Δp25-Af*pyrG; alcA-nudF-pyr4*	This paper
JZ404-405	*pyroA4*([*pyroA-gpdA*^{mini}*::GFP-RabA];* S-tagged *nudI* (or S-IC); *pyrG*89; *yA*2	This paper
JZ412	*pyroA4[pyroA-gpdA*^{mini}*::GFP-RabA];* S-tagged *nudI* (or S-IC); *alcA-nudK*^{Arp1}	This paper
JZ429	*pyroA4[pyroA-gpdA*^{mini}*::GFP-RabA];* S-tagged *nudI* (or S-IC); Δp25-Af*pyrG; pabaA*1	This paper
JZ449-452	p25-GFP-*Af*p*yrG;* S-tagged *nudM*-Af*pyrG;* possibly Δ*nkuA-argB*; possibly *pyrG*89	This paper
JZ446-448	p25-GFP-*Af*p*yrG*; *alcA*-GFP-Arp11; S-tagged *nudM*-Af*pyrG*; GFP-*nudA; pyroA4;* possibly Δ*nkuA-argB*; possibly *pyrG*89	This paper
JZ453-454	p25-GFP-*Af*p*yrG*; *alcA*-GFP-p62; S-tagged *nudM*-Af*pyrG*; GFP-*nudA;* possibly Δ*nkuA-argB*; possibly *pyrG*89	This paper
LF1	Δp25-Af*pyrG*; GFP-*nudA*; Δ*nkuA::argB*; *pyroA*4; *pyrG*89	This paper
LZ12	GFP-*nudA*; Δ*nkuA::argB*; *pyroA*4; *pyrG*89	Zhuang et al., 2007
LZ26	GFP-*nudA*; S-tagged *nudI* (or S-IC); Δ*nkuA::argB*; *pyroA*4; *pyrG*89, *yA*1	Zhuang et al., 2007
LW01	S-tagged *nudM*-Af*pyrG*; Δ*nkuA-argB*; *pyrG*89*; pyroA*4	Zhang et al., 2008
LW05	S-tagged *nudM*-Af*pyrG*; *alcA*-GFP-Arp11-*pyr4;* GFP-*nudA; pyroA4; yA*1*;* possibly Δ*nkuA-argB*; possibly *pyrG*89	Zhang et al., 2008
LW07	S-tagged *nudM*-Af*pyrG*; GFP-*nudA; pyroA4;* possibly Δ*nkuA-argB*; possibly *pyrG*89	Zhang et al., 2008
MAD2084	*inoB2; pyroA4[pyroA*-RabAp*::GFP-*RabA]*	Abenza et al., 2009
MAD2276	*yA2; pantoB*100*; argB2::[argB*-alcAp*::mCherry-*RabA]*	Zhang et al., 2010
MAD2743	*yA*2; *pyroA*4; *pantoB*100	This paper
MAD3131	*yA2; pyroA4*(*pyroA-gpdA*^{mini}*::GFP-RabA*)*; pantoB*100	This paper
TNO2A3	Δ*nkuA*::*argB*; *pyrG*89; *pyroA*4	Nayak et al., 2006
XX201	Δ*nudF-pyrG;* GFP-*nudA; argB2::[argB*-alcAp*::mCherry-*RabA]*	Zhang et al., 2010
XX222	GFP-*nudA; argB2::[argB*-alcAp*::mCherry-*RabA]; pantoB*100	This paper
XX223	Δp25-Af*pyrG*; GFP-*nudA; argB2::[argB*-alcAp*::mCherry-*RabA]*	This paper
XY13	p150-GFP-*Af*p*yrG*; Δ*nkuA*::*argB*; *pyrG*89; *pyroA*4	This paper
XY15	p150-GFP-*Af*p*yrG; alcA-nudF-pyr4; pyroA4; possibly* Δ*nkuA*::*argB*	This paper
XY27	Δp25-Af*pyrG*; p150-GFP-*Af*p*yrG; alcA-nudF-pyr4; pantoB*100*;* possibly Δ*nkuA*::*argB*	This paper
XY41	p25-GFP-*Af*p*yrG*; Δ*nkuA*::*argB*; *pyrG*89; *pyroA*4	This paper

were selected by microscopic observation of the microtubule plus-end comets, followed by Western analysis using a GFP antibody (Covance) and the p150 antibody (Zhang et al., 2008).

Construction of the p25-GFP strain

Construction of the p25-GFP fusion was done similarly to the construction of the p150-GFP fusion described above, except that the following primers were used. p25 ORF forward (5′-TATGAGCTTAGCCTGCCCCAC-3′), p25 ORF reverse (5′-TCGGATACTTCGATATCTCTCCCG-3′), fusion forward (5′-TCGGGAGAGATATCGAAGTATCCGAGGAGCTGGTGCAGGCGCTGGAG-3′), fusion reverse (5′-CCGAGGCCGACTCCAAGTACAGTACCTGTCTGAGAGGAGGCACTGATG-3′), p25 UTR forward (5′-GTACTGTACTTGGAGTCGGCCTCG-3′), and p25 UTR reverse (5′-AGATATCGCCTATTACGGACG-3′). The fusion fragment was transformed to the TNO2A3 strain (Nayak et al., 2006). Transformants were selected by microscopic observation of the microtubule plus-end comets, and presence of the p25-GFP fusion gene in the genome was verified by PCR analyses.

Construction of the GFP-RabA strain in which the GFP-RabA fusion is driven by the constitutive *gpdA*^{mini} promoter

We first constructed the plasmid p1989 containing the *gpdA*^{mini}*–gfp–rabA*^{cDNA} fusion gene linked to the *A. nidulans pyroA* gene. For making the plasmid, two primers—JFA190 5′NsiI-*rabA* and JFA191 3′XmaI-*rabA*—were synthesized. JFA190 5′NsiI-*rabA* (5′-ATGCATGAATCAACGCCCGCAAATGC-3′) contains a restriction site for NsiI (underlined), and a substitution of the second codon of *rabA* (CAT is used to replace the original GTC for creating the NsiI restriction site). JFA191 3′XmaI-*rabA* (5′-CCCGGGTTAACAGGCGCATCCCTCC-3′) contains a restriction site for XmaI (underlined). These two primers were used to amplify the *rabA*-coding region from a pGEM plasmid that contains the cDNA sequence of *rabA*, and the product was digested with the restriction enzymes NsiI and XmaI. The digested fragment was cloned into the NsiI–XmaI restriction sites in the plasmid carrying the *gpdA*^{mini}*–gfp* fusion upstream of these sites and a *gpdA* terminator downstream of these restriction sites, as well as the *A. nidulans pyroA* gene as a selection marker. The resulting plasmid, p1989, was used to transform *A. nidulans* strain MAD2743. *A. nidulans* strain MAD3131 was selected from the transformants for further studies because a Southern blot analysis on BamHI-digested genomic DNA indicates that this strain contains a single-copy integration of the plasmid at the *pyroA* locus.

Live cell imaging

Cells were grown at 32°C overnight in 0.5 ml of minimal medium with glycerol or glucose plus supplements using the Laboratory-Tek Chambered #1.0 Borosilicate Coverglass System. Images were captured at room temperature using an inverted fluorescence microscope (IX70; Olympus) with a 100× objective lens (numerical aperture, 1.35; Olympus). A cooled charge-coupled device camera (Sensicam QE; PCO/Cooke Corporation) was used. A filter wheel system with GFP/mCherry-ET Sputtered series with high transmission (BioVision Technologies) was used. The IPLab software was used for image acquisition and analysis. For GFP and mCherry images, a 100-ms exposure time was used. For measuring the signal intensity of the individual GFP-HC comets, an area containing the whole comet was selected as a region of interest (ROI), and the Max/Min tool of the IPLab program was used to measure the maximal intensity within the ROI. Then the ROI box was dragged outside of the cell to take the background value, which was then subtracted from the value of the comet. Because

comets that have arrived at the hyphal tip show the highest signal intensity, as we have described previously (Zhang et al., 2003; Efimov et al., 2006), we only selected frames within a sequence in which the comets are seen at the hyphal tip region, and only those comets that have arrived at the hyphal tip were measured. GFP-HC signals in wild type and in the Δp25 mutant were measured under the same conditions. Photoshop (Adobe) was used to process images after data acquisition. Images in Fig. 2 and Fig. 3 were processed in Photoshop to increase the brightness (wild-type and mutant images within one figure were always treated together rather than individually) so that cell shape can be seen more easily.

Biochemical analyses of dynein–early endosome interaction, p150–Arp1 interaction, and dynein–dynactin interaction

To study dynein–early endosome interaction, we took advantage of the previously constructed strains expressing S-IC (Zhuang et al., 2007), and determined if dynein can pull down GFP-RabA–associated early endosomes in the absence of detergent. We modified the previously made GFP-RabA construct so that the fusion is driven by the constitutive *gpdA*^{mini} promoter instead of the inducible *alcA* promoter (Abenza et al., 2009; Pantazopoulou and Peñalva 2009), which allows the GFP–RabA fusion to be expressed in regular rich medium instead of minimal medium with glycerol as a carbon source. This modification facilitated the biochemical analyses because cells grow much more robustly in rich medium than in glycerol-containing minimal medium. Strains containing both S-tagged dynein IC (Zhuang et al., 2007) and GFP-RabA were constructed by genetic crossing. 8 g of hyphal mass after an overnight culture was used for each experiment. Cell extracts were prepared using the buffer containing 25 mM Tris-HCl, pH 8.0, with 10 µl/ml of a protease inhibitor cocktail (Sigma-Aldrich). To ensure that we do not extract dynein away from the membranous vesicles, no detergent was added to the buffer. Also, to ensure that most membranous vesicles are in the extract for pull-down assays, only a low-speed spin (4,000 *g*) was performed to remove cell debris. The extracts were incubated with S-agarose beads, followed by gentle washing and then elution with 10 mg/ml of S-peptide in 25 mM Tris-HCl, pH 8.0, containing 10 µl/ml of a protease inhibitor cocktail (Sigma-Aldrich). Dynein IC and GFP-RabA were detected using an anti-IC antibody (Zhang et al., 2008) and an anti-GFP antibody (Takara Bio Inc.). Western analyses were performed using the alkaline phosphatase system, and blots were developed using the AP color development reagents from Bio-Rad Laboratories. Protein band intensity was measured using the IPlab software. Specifically, the blots were scanned and saved as TIF files. The images were inverted using the IPlab software, the intensity at three representative positions of a band was measured, and the mean of these three values was calculated. The background values were measured at three different positions of the same blot in between lanes, and the mean background value was subtracted from the intensity values of the bands. The S-tagged dynein IC band was used as an internal control, and the ratio of pulled-down GFP-RabA to S-tagged IC was calculated. The ratios calculated from the wild-type samples were set as 1, and the relative values of the mutants were calculated and presented.

Analyses of p150–Arp1 interaction, p150–p25 interaction, and dynein–dynactin interaction were done using a strain containing a functional S-tagged p150 (Zhang et al., 2008). The Δp25 allele or the p25-GFP allele was introduced into this strain background by genetic crossing, and the presence of the p25 deletion or the p25-GFP fusion gene in the genome was determined by PCR analyses of the genomic DNA. Protein isolation and pull-down assays were performed using the low-salt Tris buffer (25 mM Tris-HCl, pH 8.0, and 0.4% Triton-X-100), as described previously (Zhang et al., 2008). Antibodies against p150, Arp1, and dynein heavy chain have been described previously (Xiang et al., 1995; Zhang et al., 2008), and the anti-GFP antibody we used for this study was from Takara Bio Inc.

Online supplemental material

Fig. S1 shows site-specific integration of the Δp25 construct into the genome of the Δp25 mutant as indicated by PCR and Southern blot analyses. Fig. S2 shows that S-tagged p150 (S-p150) pulled down a normal amount of Arp1 from Δp25 cell extract but not from *alcA*-Arp11 cell extract. Fig. S3 shows that dynein–dynactin interaction is not negatively affected by loss of p25. Video 1 shows bidirectional movements of early endosomes labeled by mCherry-RabA in a wild-type hypha. Videos 2 and 3 show that early endosomes in Δp25 hyphae are largely accumulated at the hyphal tip. Video 4 shows that early endosomes in a Δ*nudA* (dynein heavy chain) hypha are largely accumulated at the hyphal tip. Video 5 shows GFP-dynein HC (GFP-HC) signals in the Δ*nudF* mutant. Video 6 shows mCherry-RabA signals in the same Δ*nudF* cells shown in Video 5. Video 7 shows a merge of the GFP-HC and mCherry-RabA signals in the same Δ*nudF* mutant cells as shown in Videos 5 and 6. Video 8 shows a cloud-like structure at the hyphal tip formed by p150-GFP in *alcA-nudF* cells. Online supplemental material is available at http://www.jcb.org/cgi/content/full/jcb.201011022/DC1.

We thank Berl Oakley for the Δ*nkuA* strain, the Fungal Genetic Stock Center (FGSC) for pAO81 and pFNO3 plasmids, and Steve Osmani for depositing them. We thank the reviewers for suggestions that helped us to improve the work and its presentation.

This work was supported by the National Institutes of Health (GM069527 to X. Xiang), Comprehensive Neuroscience Program (CNP)/Department of Defense (to X. Xiang), the Center for Neuroscience and Regenerative Medicine (CNRM)/Department of Defense at Uniformed Services University of the Health Sciences (to X. Xiang), a Uniformed Services University of the Health Sciences intramural grant (to X. Xiang), the Uniformed Services University Center for Health Disparities (to L. Fischer), DGICYT BIO2009-07281 (to M.A. Peñalva), and Comunidad de Madrid S2006-SAL-0246 (to M.A. Peñalva). J.F. Abenza is holder of a Consejo Superior de Investigaciones Cientificas I3P predoctoral contract.

Submitted: 3 November 2010
Accepted: 6 June 2011

References

Abenza, J.F., A. Pantazopoulou, J.M. Rodríguez, A. Galindo, and M.A. Peñalva. 2009. Long-distance movement of *Aspergillus nidulans* early endosomes on microtubule tracks. *Traffic*. 10:57–75. doi:10.1111/j.1600-0854.2008.00848.x

Abenza, J.F., A. Galindo, A. Pantazopoulou, C. Gil, V. de los Ríos, and M.A. Peñalva. 2010. *Aspergillus* RabB Rab5 integrates acquisition of degradative identity with the long distance movement of early endosomes. *Mol. Biol. Cell*. 21:2756–2769. doi:10.1091/mbc.E10-02-0119

Akhmanova, A., and J.A. Hammer III. 2010. Linking molecular motors to membrane cargo. *Curr. Opin. Cell Biol.* 22:479–487. doi:10.1016/j.ceb.2010.04.008

Araujo-Bazán, L., M.A. Peñalva, and E.A. Espeso. 2008. Preferential localization of the endocytic internalization machinery to hyphal tips underlies polarization of the actin cytoskeleton in *Aspergillus nidulans*. *Mol. Microbiol.* 67:891–905. doi:10.1111/j.1365-2958.2007.06102.x

Borkovich, K.A., L.A. Alex, O. Yarden, M. Freitag, G.E. Turner, N.D. Read, S. Seiler, D. Bell-Pedersen, J. Paietta, N. Plesofsky, et al. 2004. Lessons from the genome sequence of *Neurospora crassa*: tracing the path from genomic blueprint to multicellular organism. *Microbiol. Mol. Biol. Rev.* 68:1–108. doi:10.1128/MMBR.68.1.1-108.2004

Cai, Q., L. Lu, J.H. Tian, Y.B. Zhu, H. Qiao, and Z.H. Sheng. 2010. Snapin-regulated late endosomal transport is critical for efficient autophagy-lysosomal function in neurons. *Neuron*. 68:73–86. doi:10.1016/j.neuron.2010.09.022

Caviston, J.P., and E.L. Holzbaur. 2006. Microtubule motors at the intersection of trafficking and transport. *Trends Cell Biol.* 16:530–537. doi:10.1016/j.tcb.2006.08.002

Clark, S.W., and M.D. Rose. 2006. Arp10p is a pointed-end-associated component of yeast dynactin. *Mol. Biol. Cell*. 17:738–748. doi:10.1091/mbc.E05-05-0449

Culver-Hanlon, T.L., S.A. Lex, A.D. Stephens, N.J. Quintyne, and S.J. King. 2006. A microtubule-binding domain in dynactin increases dynein processivity by skating along microtubules. *Nat. Cell Biol.* 8:264–270. doi:10.1038/ncb1370

Delcroix, J.D., J.S. Valletta, C. Wu, S.J. Hunt, A.S. Kowal, and W.C. Mobley. 2003. NGF signaling in sensory neurons: evidence that early endosomes carry NGF retrograde signals. *Neuron*. 39:69–84. doi:10.1016/S0896-6273(03)00397-0

Dixit, R., J.R. Levy, M. Tokito, L.A. Ligon, and E.L. Holzbaur. 2008. Regulation of dynactin through the differential expression of p150Glued isoforms. *J. Biol. Chem.* 283:33611–33619. doi:10.1074/jbc.M804840200

Eckley, D.M., S.R. Gill, K.A. Melkonian, J.B. Bingham, H.V. Goodson, J.E. Heuser, and T.A. Schroer. 1999. Analysis of dynactin subcomplexes reveals a novel actin-related protein associated with the arp1 minifilament pointed end. *J. Cell Biol.* 147:307–320. doi:10.1083/jcb.147.2.307

Efimov, V.P., J. Zhang, and X. Xiang. 2006. CLIP-170 homologue and NUDE play overlapping roles in NUDF localization in *Aspergillus nidulans*. *Mol. Biol. Cell*. 17:2021–2034. doi:10.1091/mbc.E05-11-1084

Fejtova, A., D. Davydova, F. Bischof, V. Lazarevic, W.D. Altrock, S. Romorini, C. Schöne, W. Zuschratter, M.R. Kreutz, C.C. Garner, et al. 2009. Dynein light chain regulates axonal trafficking and synaptic levels of Bassoon. *J. Cell Biol.* 185:341–355. doi:10.1083/jcb.200807155

Haghnia, M., V. Cavalli, S.B. Shah, K. Schimmelpfeng, R. Brusch, G. Yang, C. Herrera, A. Pilling, and L.S. Goldstein. 2007. Dynactin is required for coordinated bidirectional motility, but not for dynein membrane attachment. *Mol. Biol. Cell*. 18:2081–2089. doi:10.1091/mbc.E06-08-0695

Han, G., B. Liu, J. Zhang, W. Zuo, N.R. Morris, and X. Xiang. 2001. The *Aspergillus* cytoplasmic dynein heavy chain and NUDF localize to microtubule ends and affect microtubule dynamics. *Curr. Biol.* 11:719–724. doi:10.1016/S0960-9822(01)00200-7

Harris, S.D. 2010. Hyphal growth and polarity. *In* Cellular and Molecular Biology of Filamentous Fungi. K. Borkovich and D. Ebbole, editors. ASM Press, Washington, D.C. 238–259.

Hervás-Aguilar, A., and M.A. Peñalva. 2010. Endocytic machinery protein SlaB is dispensable for polarity establishment but necessary for polarity maintenance in hyphal tip cells of *Aspergillus nidulans*. *Eukaryot. Cell*. 9:1504–1518. doi:10.1128/EC.00119-10

Hodgkinson, J.L., C. Peters, S.A. Kuznetsov, and W. Steffen. 2005. Three-dimensional reconstruction of the dynactin complex by single-particle image analysis. *Proc. Natl. Acad. Sci. USA*. 102:3667–3672. doi:10.1073/pnas.0409506102

Holleran, E.A., M.K. Tokito, S. Karki, and E.L. Holzbaur. 1996. Centractin (ARP1) associates with spectrin revealing a potential mechanism to link dynactin to intracellular organelles. *J. Cell Biol.* 135:1815–1829. doi:10.1083/jcb.135.6.1815

Holleran, E.A., L.A. Ligon, M. Tokito, M.C. Stankewich, J.S. Morrow, and E.L. Holzbaur. 2001. beta III spectrin binds to the Arp1 subunit of dynactin. *J. Biol. Chem.* 276:36598–36605. doi:10.1074/jbc.M104838200

Horgan, C.P., S.R. Hanscom, R.S. Jolly, C.E. Futter, and M.W. McCaffrey. 2010. Rab11-FIP3 links the Rab11 GTPase and cytoplasmic dynein to mediate transport to the endosomal-recycling compartment. *J. Cell Sci.* 123:181–191. doi:10.1242/jcs.052670

Imai, H., A. Narita, T.A. Schroer, and Y. Maéda. 2006. Two-dimensional averaged images of the dynactin complex revealed by single particle analysis. *J. Mol. Biol.* 359:833–839. doi:10.1016/j.jmb.2006.03.071

Johansson, M., N. Rocha, W. Zwart, I. Jordens, L. Janssen, C. Kuijl, V.M. Olkkonen, and J. Neefjes. 2007. Activation of endosomal dynein motors by stepwise assembly of Rab7-RILP-p150Glued, ORP1L, and the receptor betalll spectrin. *J. Cell Biol.* 176:459–471. doi:10.1083/jcb.200606077

Kardon, J.R., and R.D. Vale. 2009. Regulators of the cytoplasmic dynein motor. *Nat. Rev. Mol. Cell Biol.* 10:854–865. doi:10.1038/nrm2804

Kardon, J.R., S.L. Reck-Peterson, and R.D. Vale. 2009. Regulation of the processivity and intracellular localization of *Saccharomyces cerevisiae* dynein by dynactin. *Proc. Natl. Acad. Sci. USA*. 106:5669–5674. doi:10.1073/pnas.0900976106

Karki, S., and E.L. Holzbaur. 1995. Affinity chromatography demonstrates a direct binding between cytoplasmic dynein and the dynactin complex. *J. Biol. Chem.* 270:28806–28811. doi:10.1074/jbc.270.48.28806

Kim, H., S.C. Ling, G.C. Rogers, C. Kural, P.R. Selvin, S.L. Rogers, and V.I. Gelfand. 2007. Microtubule binding by dynactin is required for microtubule organization but not cargo transport. *J. Cell Biol.* 176:641–651. doi:10.1083/jcb.200608128

King, S.J., and T.A. Schroer. 2000. Dynactin increases the processivity of the cytoplasmic dynein motor. *Nat. Cell Biol.* 2:20–24. doi:10.1038/71338

Lee, I.H., S. Kumar, and M. Plamann. 2001. Null mutants of the neurospora actin-related protein 1 pointed-end complex show distinct phenotypes. *Mol. Biol. Cell*. 12:2195–2206.

Lee, W.L., J.R. Oberle, and J.A. Cooper. 2003. The role of the lissencephaly protein Pac1 during nuclear migration in budding yeast. *J. Cell Biol.* 160:355–364. doi:10.1083/jcb.200209022

Lenz, J.H., I. Schuchardt, A. Straube, and G. Steinberg. 2006. A dynein loading zone for retrograde endosome motility at microtubule plus-ends. *EMBO J.* 25:2275–2286. doi:10.1038/sj.emboj.7601119

Lomakin, A.J., I. Semenova, I. Zaliapin, P. Kraikivski, E. Nadezhdina, B.M. Slepchenko, A. Akhmanova, and V. Rodionov. 2009. CLIP-170-dependent capture of membrane organelles by microtubules initiates minus-end directed transport. *Dev. Cell*. 17:323–333. doi:10.1016/j.devcel.2009.07.010

Lorenzo, D.N., M.G. Li, S.E. Mische, K.R. Armbrust, L.P. Ranum, and T.S. Hays. 2010. Spectrin mutations that cause spinocerebellar ataxia type 5 impair axonal transport and induce neurodegeneration in *Drosophila*. *J. Cell Biol.* 189:143–158. doi:10.1083/jcb.200905158

Ma, L., M.Y. Tsai, S. Wang, B. Lu, R. Chen, J.R. Iii, X. Zhu, and Y. Zheng. 2009. Requirement for Nudel and dynein for assembly of the lamin B spindle matrix. *Nat. Cell Biol.* 11:247–256. doi:10.1038/ncb1832

McCluskey, K., A. Wiest, and M. Plamann. 2010. The Fungal Genetics Stock Center: a repository for 50 years of fungal genetics research. *J. Biosci.* 35:119–126. doi:10.1007/s12038-010-0014-6

Minke, P.F., I.H. Lee, J.H. Tinsley, K.S. Bruno, and M. Plamann. 1999. Neurospora crassa ro-10 and ro-11 genes encode novel proteins required for nuclear distribution. *Mol. Microbiol.* 32:1065–1076. doi:10.1046/j.1365-2958.1999.01421.x

Moore, J.K., J. Li, and J.A. Cooper. 2008. Dynactin function in mitotic spindle positioning. *Traffic*. 9:510–527. doi:10.1111/j.1600-0854.2008.00710.x

Moore, J.K., D. Sept, and J.A. Cooper. 2009a. Neurodegeneration mutations in dynactin impair dynein-dependent nuclear migration. *Proc. Natl. Acad. Sci. USA*. 106:5147–5152. doi:10.1073/pnas.0810828106

Moore, J.K., M.D. Stuchell-Brereton, and J.A. Cooper. 2009b. Function of dynein in budding yeast: mitotic spindle positioning in a polarized cell. *Cell Motil. Cytoskeleton*. 66:546–555. doi:10.1002/cm.20364

Morris, N.R. 2000. Nuclear migration. From fungi to the mammalian brain. *J. Cell Biol.* 148:1097–1101. doi:10.1083/jcb.148.6.1097

Muresan, V., M.C. Stankewich, W. Steffen, J.S. Morrow, E.L. Holzbaur, and B.J. Schnapp. 2001. Dynactin-dependent, dynein-driven vesicle transport in the absence of membrane proteins: a role for spectrin and acidic phospholipids. *Mol. Cell*. 7:173–183. doi:10.1016/S1097-2765(01)00165-4

Nayak, T., E. Szewczyk, C.E. Oakley, A. Osmani, L. Ukil, S.L. Murray, M.J. Hynes, S.A. Osmani, and B.R. Oakley. 2006. A versatile and efficient gene-targeting system for *Aspergillus nidulans*. *Genetics*. 172:1557–1566. doi:10.1534/genetics.105.052563

Pantazopoulou, A., and M.A. Peñalva. 2009. Organization and dynamics of the *Aspergillus nidulans* Golgi during apical extension and mitosis. *Mol. Biol. Cell*. 20:4335–4347. doi:10.1091/mbc.E09-03-0254

Parisi, G., M.S. Fornasari, and J. Echave. 2004. Dynactins p25 and p27 are predicted to adopt the LbetaH fold. *FEBS Lett.* 562:1–4. doi:10.1016/S0014-5793(04)00165-6

Peñalva, M.A. 2010. Endocytosis in filamentous fungi: Cinderella gets her reward. *Curr. Opin. Microbiol.* 13:684–692. doi:10.1016/j.mib.2010.09.005

Perlson, E., S. Maday, M.M. Fu, A.J. Moughamian, and E.L. Holzbaur. 2010. Retrograde axonal transport: pathways to cell death? *Trends Neurosci.* 33:335–344. doi:10.1016/j.tins.2010.03.006

Schafer, D.A., S.R. Gill, J.A. Cooper, J.E. Heuser, and T.A. Schroer. 1994. Ultrastructural analysis of the dynactin complex: an actin-related protein is a component of a filament that resembles F-actin. *J. Cell Biol.* 126:403–412. doi:10.1083/jcb.126.2.403

Schroer, T.A. 2004. Dynactin. *Annu. Rev. Cell Dev. Biol.* 20:759–779. doi:10.1146/annurev.cellbio.20.012103.094623

Schuster, M., S. Kilaru, P. Ashwin, C. Lin, N.J. Severs, and G. Steinberg. 2011a. Controlled and stochastic retention concentrates dynein at microtubule ends to keep endosomes on track. *EMBO J.* 30:652–664. doi:10.1038/emboj.2010.360

Schuster, M., R. Lipowsky, M.A. Assmann, P. Lenz, and G. Steinberg. 2011b. Transient binding of dynein controls bidirectional long-range motility of early endosomes. *Proc. Natl. Acad. Sci. USA*. 108:3618–3623. doi:10.1073/pnas.1015839108

Sheeman, B., P. Carvalho, I. Sagot, J. Geiser, D. Kho, M.A. Hoyt, and D. Pellman. 2003. Determinants of *S. cerevisiae* dynein localization and activation: implications for the mechanism of spindle positioning. *Curr. Biol.* 13:364–372. doi:10.1016/S0960-9822(03)00013-7

Soldati, T., and M. Schliwa. 2006. Powering membrane traffic in endocytosis and recycling. *Nat. Rev. Mol. Cell Biol.* 7:897–908. doi:10.1038/nrm2060

Starr, D.A., B.C. Williams, T.S. Hays, and M.L. Goldberg. 1998. ZW10 helps recruit dynactin and dynein to the kinetochore. *J. Cell Biol.* 142:763–774. doi:10.1083/jcb.142.3.763

Steinberg, G. 2007. On the move: endosomes in fungal growth and pathogenicity. *Nat. Rev. Microbiol.* 5:309–316. doi:10.1038/nrmicro1618

Steinberg, G., and M. Schuster. 2011. The dynamic fungal cell. *Fungal Biol. Rev.* 25:14–37. doi:10.1016/j.fbr.2011.01.008

Szewczyk, E., T. Nayak, C.E. Oakley, H. Edgerton, Y. Xiong, N. Taheri-Talesh, S.A. Osmani, and B.R. Oakley. 2006. Fusion PCR and gene targeting in *Aspergillus nidulans*. *Nat. Protoc.* 1:3111–3120. (published erratum appears in *Nat. Protoc*. 2006. 1:31120) doi:10.1038/nprot.2006.405

Taheri-Talesh, N., T. Horio, L. Araujo-Bazán, X. Dou, E.A. Espeso, M.A. Peñalva, S.A. Osmani, and B.R. Oakley. 2008. The tip growth apparatus of *Aspergillus nidulans*. *Mol. Biol. Cell*. 19:1439–1449. doi:10.1091/mbc.E07-05-0464

Tai, A.W., J.Z. Chuang, C. Bode, U. Wolfrum, and C.H. Sung. 1999. Rhodopsin's carboxy-terminal cytoplasmic tail acts as a membrane receptor for cytoplasmic dynein by binding to the dynein light chain Tctex-1. *Cell*. 97:877–887. doi:10.1016/S0092-8674(00)80800-4

Upadhyay, S., and B.D. Shaw. 2008. The role of actin, fimbrin and endocytosis in growth of hyphae in *Aspergillus nidulans*. *Mol. Microbiol.* 68:690–705. doi:10.1111/j.1365-2958.2008.06178.x

Vallee, R.B., D. Varma, and D.L. Dujardin. 2006. ZW10 function in mitotic checkpoint control, dynein targeting and membrane trafficking: is dynein the unifying theme? *Cell Cycle*. 5:2447–2451. doi:10.4161/cc.5.21.3395

Vaughan, K.T., and R.B. Vallee. 1995. Cytoplasmic dynein binds dynactin through a direct interaction between the intermediate chains and p150Glued. *J. Cell Biol.* 131:1507–1516. doi:10.1083/jcb.131.6.1507

Whyte, J., J.R. Bader, S.B. Tauhata, M. Raycroft, J. Hornick, K.K. Pfister, W.S. Lane, G.K. Chan, E.H. Hinchcliffe, P.S. Vaughan, and K.T. Vaughan. 2008. Phosphorylation regulates targeting of cytoplasmic dynein to kinetochores during mitosis. *J. Cell Biol.* 183:819–834. doi:10.1083/jcb.200804114

Xiang, X., and B.R. Oakley. 2010. The cytoskeleton in filamentous fungi. *In* Cellular and Molecular Biology of Filamentous Fungi. K. Borkovich and D. Ebbole, editors. ASM Press, Washington, D.C. 209–223.

Xiang, X., C. Roghi, and N.R. Morris. 1995. Characterization and localization of the cytoplasmic dynein heavy chain in *Aspergillus nidulans. Proc. Natl. Acad. Sci. USA*. 92:9890–9894. doi:10.1073/pnas.92.21.9890

Yang, L., L. Ukil, A. Osmani, F. Nahm, J. Davies, C.P. De Souza, X. Dou, A. Perez-Balaguer, and S.A. Osmani. 2004. Rapid production of gene replacement constructs and generation of a green fluorescent protein-tagged centromeric marker in *Aspergillus nidulans*. *Eukaryot. Cell*. 3:1359–1362. doi:10.1128/EC.3.5.1359-1362.2004

Yeh, E., R.V. Skibbens, J.W. Cheng, E.D. Salmon, and K. Bloom. 1995. Spindle dynamics and cell cycle regulation of dynein in the budding yeast, *Saccharomyces cerevisiae. J. Cell Biol.* 130:687–700. doi:10.1083/jcb.130.3.687

Zekert, N., and R. Fischer. 2009. The *Aspergillus nidulans* kinesin-3 UncA motor moves vesicles along a subpopulation of microtubules. *Mol. Biol. Cell*. 20:673–684. doi:10.1091/mbc.E08-07-0685

Zhang, J., S. Li, R. Fischer, and X. Xiang. 2003. Accumulation of cytoplasmic dynein and dynactin at microtubule plus ends in *Aspergillus nidulans* is kinesin dependent. *Mol. Biol. Cell*. 14:1479–1488. doi:10.1091/mbc.E02-08-0516

Zhang, J., L. Wang, L. Zhuang, L. Huo, S. Musa, S. Li, and X. Xiang. 2008. Arp11 affects dynein-dynactin interaction and is essential for dynein function in *Aspergillus nidulans. Traffic*. 9:1073–1087. doi:10.1111/j.1600-0854.2008.00748.x

Zhang, J., L. Zhuang, Y. Lee, J.F. Abenza, M.A. Peñalva, and X. Xiang. 2010. The microtubule plus-end localization of *Aspergillus* dynein is important for dynein-early-endosome interaction but not for dynein ATPase activation. *J. Cell Sci.* 123:3596–3604. doi:10.1242/jcs.075259

Zhuang, L., J. Zhang, and X. Xiang. 2007. Point mutations in the stem region and the fourth AAA domain of cytoplasmic dynein heavy chain partially suppress the phenotype of NUDF/LIS1 loss in *Aspergillus nidulans*. *Genetics*. 175:1185–1196. doi:10.1534/genetics.106.069013